SHARE4.0

PILOT ACTION REPORT

WP3 – D3.3.1.3

Version 1
FOTEC – Christoph Ackerl, Martin Braunstorfer
UMMS – Lubomir Orovcik
Date 25.09.2022

Table of contents

1 Part description

The test component is a fuel collector from an engine of a small aircraft. Currently, it is an assembly of five individual parts that are welded manually due to the small number of pieces. For certification as a critical aerospace component, each weld must be inspected manually to ensure proper function. The original component in the installed state in the engine (left) and as a single component (right) is shown in Figure 1.

The five individual parts of stainless steel have a total weight of 43.7 g and a volume of 5,425 mm³ when welded together.

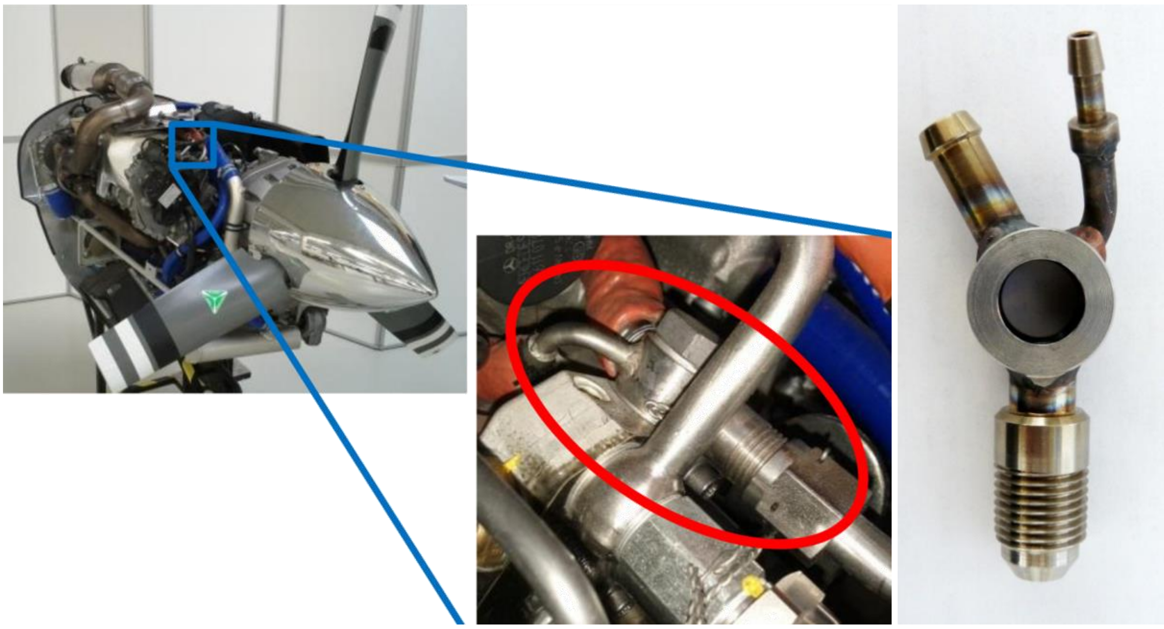

Figure 1: mounting position of fuel collector

2 Functional optimization and preparation for laser beam melting

Analogous to the criteria catalog, the benefits of additive manufacturing for the component were first investigated. It turns out that both a significantly lighter construction method and a monolithic design can be applied. At the beginning, the component was digitized via CAD (computer aided design), since no complete assembly model was available. Figure 2 shows the Constructive implementation as a 3D model in the CAD software.

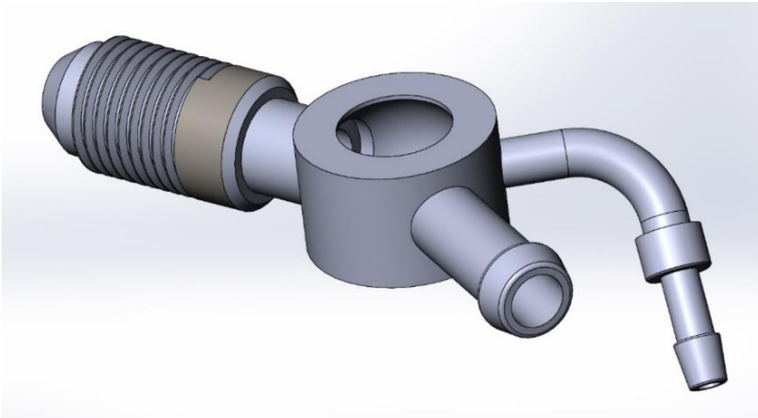

Figure 2: reconstruction of the original part

The next step is to analyze which conditions and substances the component is exposed to. The original component is made of a chrome-nickel alloy, as this is corrosion-resistant and can be easily joined using the TIG welding process. Several analyses have shown that the titanium alloy Ti6Al4V, which is widely used in additive manufacturing, has sufficient resistance. In addition, it has the advantage that the physical density is significantly lower than that of the starting material, which means that significant mass savings can be achieved only by using this alloy.

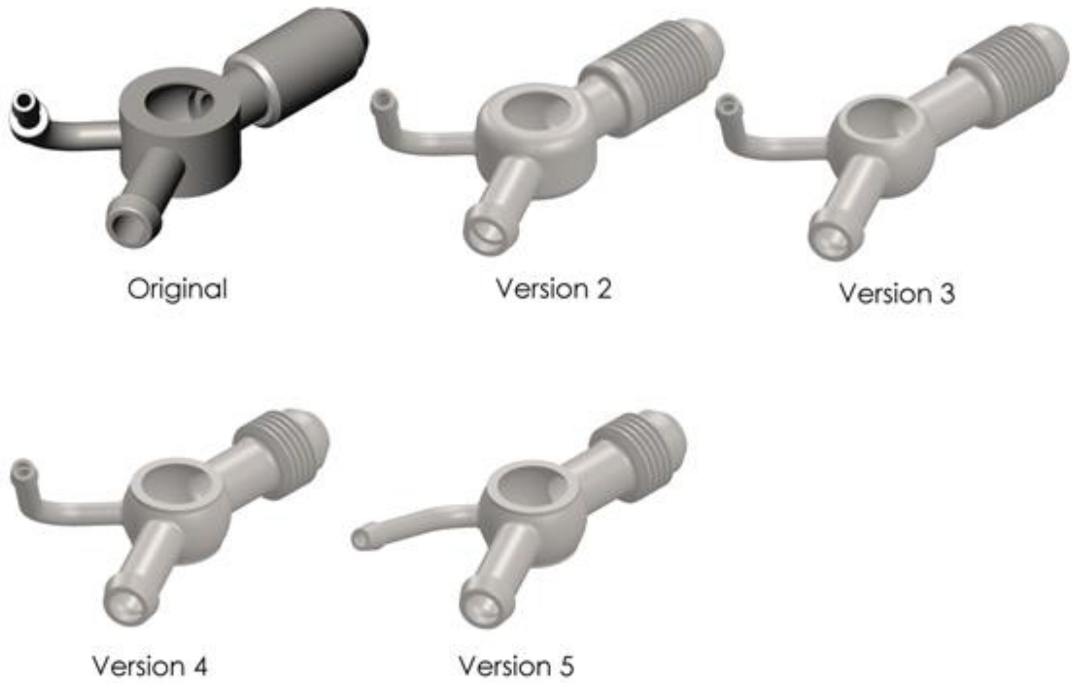

Figure 3: optimization steps of fuel collector

2.1 Version 2: mass and weight

The weight saving due to the change of materials is considerable. The original component has a weight of approx. 43 g. If the same geometry is made of Ti6Al4V, the weight would be reduced to 23.9 g, which corresponds to a reduction of 44.2 %.

In a first optimization step, the wall thicknesses in the central ring element are reduced, since the high wall thickness in the original part served mainly to orient the welded-on components. In addition, several edges are rounded, as can be seen in Figure 3 as version 2. The reduction in wall thickness further reduces the weight of the part to 19.4 g, which is roughly a court reduction of 54.6 % in comparison to the original component.

2.2 Version 3: thread length

As the next step, the installation situation of the component was analyzed for a functional optimization. The result of the investigations was that the thread length can be reduced. In addition, the middle sector can be reshaped so that the volume can also be further reduced. These modifications result in version 3, which can be seen in Figure 3. This further reduces the weight to 12 g, which corresponds to a reduction of approx. 72 % compared to the original part.

2.3 Version 4: sealing and tightness

In version 4, the sealing surface of the central part has been enlarged to ensure a better tightness. Furthermore, the thread length could be further reduced, as a secure connection with the fitting can also be made with this thread length (see Figure 3 as Version 4). The weight could be further reduced and is 11 g for this version, which corresponds to a reduction of 74 % compared to the original weight.

2.4 Version 5: rerouting of side arm

After consultation with the engine manufacturer, an adjustment of the thinner side arm can be made. The concrete changes can be seen in Figure 3 as Version 5. These adaptions result in several advantages. First, the component volume can be further reduced, from this the weight is further reduced and now amounts to ≈10.8 g, which corresponds to a weight reduction of 75.3 %. Additionally, by adjusting the geometry, the required footprint on the build platform of the LBM system is reduced, which means that more components can be produced at the same time. Figure 4 shows the original component and the manufactured version 5.

Figure 4: original welded part in comparison to LBM manufactured version 5

2.5 Version 6: rework of functional surfaces

A closer look at the large hole in the middle section shows that the wall thickness was chosen too thin and the material has partially broken out. For this reason, the wall thickness is increased in this area in version 6. Another reason is the need for mechanical reworking of these areas to improve the surface roughness and thus ensure the tightness of this area. Figure 5 clearly shows the differences between version 5 and version 6. In addition to the allowance for the functional surfaces, the internal edges were also rounded in order to achieve a flow optimization for the propellant. Thickening the functional surfaces in version 6 increases the weight of the component by 0.2 g. Thus, the weight saving also decreases slightly to 74.8 %.

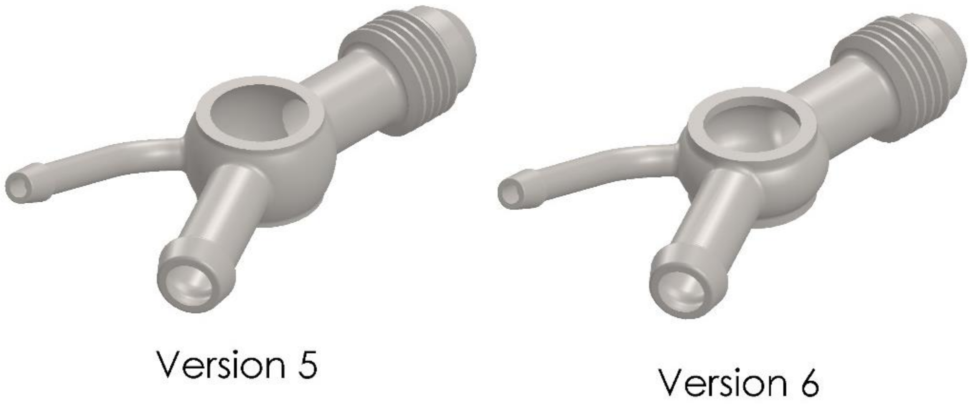

Figure 5: version 5 in comparison to version 6

3 Optimization using simulation

The optimization steps performed so far are based purely on experience and have been carried out without simulation software. The following versions are simulated using "Ansys Discovery" software and the results are verified with the integrated "fluid dynamics tool". The original design is initially used as the baseline, since the weight optimization measures already carried out could theoretically have a negative effect on the flow behavior of the fuel (see Figure 6). The lower the pressure drop, the more streamlined the geometry designed to be. The aim of the optimization is to keep this pressure drop as low as possible. To achieve qualitative results, it is important to know the flow properties of the fuel, as these can vary significantly with increasing pressures, temperatures and surface properties of the component.

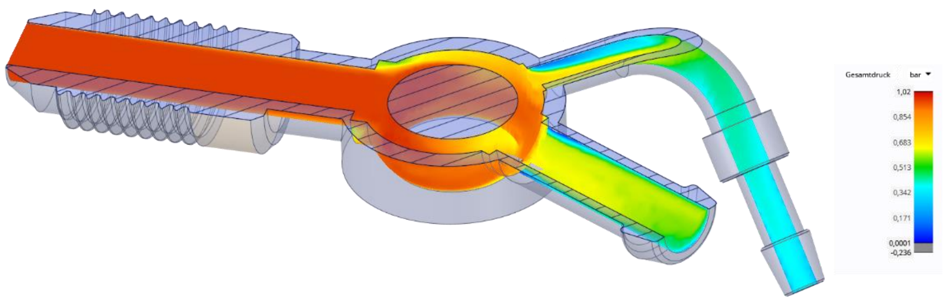

Figure 6: Flow simulation of original part – cutaway view

The simulation is based on the pressure drop of the propellant created when passing the collector. The pressure drop is always measured at both ports (see Figure 7).

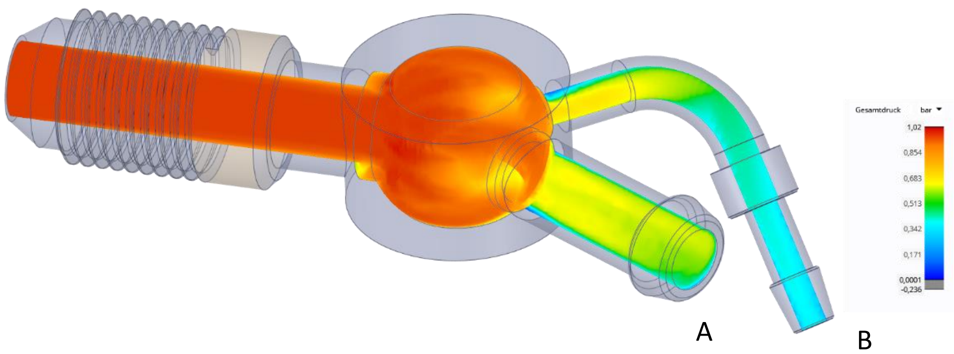

Figure 7: Flow simulation of original part with marked ports A and B

Based on an inlet pressure of 1 bar, the original version of the component reduces the outlet pressure at port A to 0.53 bar and at port B to 0.37 bar.

3.1 Version 8: simulations and optimizations

From version 6 onwards, the component was optimized in several iteration steps with the help of the simulation results. Version 8 and the final version 12 are given as examples, since the intermediate versions differ only marginally as can be seen in Table 1. The result of various simulations and optimizations of temperature, frequency simulation for rocket start and clamping forces for different load cases culminates in version 8. The weight could be further reduced and is 10.4 g for this version, which corresponds to a reduction of 76.2 % compared to the original weight. The flow simulation of this version is shown in Figure 8.

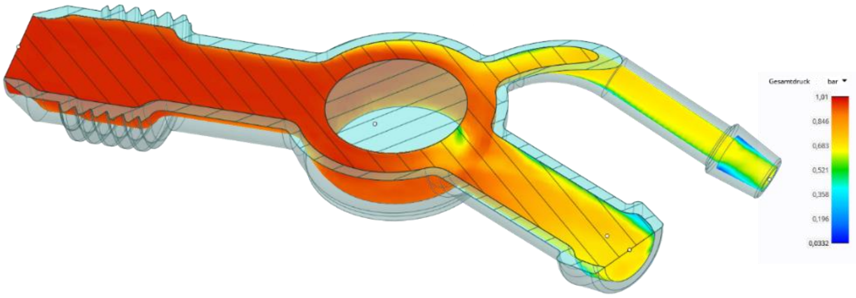

Figure 8: Flow simulation of version 8 - cutaway view

With the same inlet pressure of 1 bar, the outlet pressure of version 8 at port A now drops significantly less to 0.69 bar. Likewise, the propellant escapes at port B at a much higher pressure, namely 0.64 bar. This is almost double the pressure of the original part. In version 8, there is still a zone in the large bore where the pressure is noticeably lower. This area will be given increased attention in the next optimization steps. In addition, the pressure difference between the inlet and the two outlets is to be further reduced.

Table 1: Comparison of the weights and volumes of the different versions

Material					1.4305, 1.4301 X8CrNiS 18-9, X5CrNi 18-10	Ti64 Ti6Al4V		MS1 1.2709 X3NiCoMoTi 18-9-5	IN718 2.4668 NiCr19Fe19NbMo3	AlSi10Mg
kleinste Wandstärke (gem. Datenblatt)						ca. 0,3 – 0,4 mm		ca. 0,3 – 0,4 mm	typ. 0,3 – 0,4 mm	ca. 0,3 – 0,4 mm
Dichte (gem. Datenblatt)					7,9 kg/dm³	ca. 4,41 g/cm³		8,0 – 8,1 g/cm³	min. 8,15 g/cm³	ca. 2,68 g/cm³
Dichte (für Rechnung)					**7,90 g/cm³**	**4,41 g/cm³**		**8,05 g/cm³**	**8,15 g/cm³**	**2,68 g/cm³**
Version	**Zeichnungsnummer**	**Datum**	**Volumen**	**Volumen-Reduktion**	**Gewicht**	**Gewicht**	**Gewichts-Reduktion**	**Gewicht**	**Gewicht**	**Gewicht**
Originalteil	E4A-33-400-000 Rev. 10		5 425,1 mm³	0,0%	**42,858 g**	23,9 g	-44,2%	43,7 g	44,2 g	14,5 g
2. Version verrundet	2011-01-05 02-000	21.02.2012	4 408,8 mm³	-18,7%	34,8 g	19,4 g	-54,6%	35,5 g	35,9 g	11,8 g
3. Version neu aufgebaut	2011-01-05 03-000	22.02.2012	2 731,9 mm³	-49,6%	21,6 g	12,0 g	-71,9%	22,0 g	22,3 g	7,3 g
4. Version	2011-01-05 04-000	27.02.2012	2 499,0 mm³	-53,9%	19,7 g	11,0 g	-74,3%	20,1 g	20,4 g	6,7 g
Neue Vorgaben von Hersteller	E4A-33-400-000 Rev. 30	28.02.2012	5 583,9 mm³	0,0%	**43,722 g**	24,6 g	-43,7%	45,0 g	45,5 g	15,0 g
5.Version	2011-01-05 05-000	07.03.2012	2 450,9 mm³	-56,1%	19,4 g	10,8 g	-75,3%	19,7 g	20,0 g	6,6 g
6.Version	2011-01-05 06-000	14.03.2012	2 494,0 mm³	-55,3%	19,7 g	11,0 g	-74,8%	20,1 g	20,3 g	6,7 g
7.Version	2011-01-05 07-000	22.05.2012	2 498,2 mm³	-55,3%	19,7 g	11,0 g	-74,8%	20,1 g	20,4 g	6,7 g
8. Version	2011-01-05 08-001	19.06.2012	2 358,5 mm³	-57,8%	18,6 g	10,4 g	-76,2%	19,0 g	19,2 g	6,3 g
9. Version	2011-01-05 09-001	27.06.2012	2 358,5 mm³	-57,8%	18,6 g	10,4 g	-76,2%	19,0 g	19,2 g	6,3 g
10. Version	2011-01-05 10-001	04.07.2012	2 385,1 mm³	-57,3%	18,8 g	10,5 g	-75,9%	19,2 g	19,4 g	6,4 g
11.Version	2011-01-05 11-001	05.07.2012	2 285,7 mm³	-59,1%	18,1 g	10,1 g	-76,9%	18,4 g	18,6 g	6,1 g
12.Version	2011-01-05 12-001	05.07.2012	2 268,3 mm³	-59,4%	17,9 g	10,0 g	-77,1%	18,3 g	18,5 g	6,1 g
			Verschweißte Originalteile							

3.2 Version 12: finding and optimizing the ideal design

Table 1 shows very clearly that the volume reduction from version 9 to version 12 is only marginal. For this reason, the evolution of this is summarized in this chapter. The final CAD model of version 12 can be seen in Figure 9. The weight reduction is now 77.1 % which results in a final weight of 10.0 g.

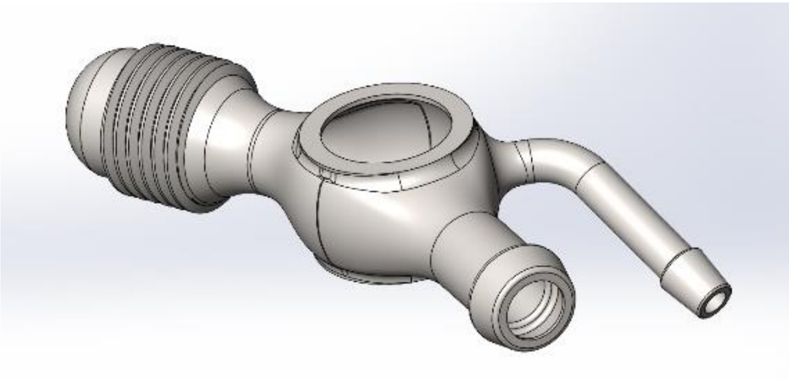

Figure 9: CAD model of version 12

Figure 10 shows a section through the flow simulation of final version 12. It is clearly visible here, that the zone in which version 8 has a large pressure drop, as can be seen at the green section in Figure 8, has been significantly improved. Starting from the original part, the pressure drop at both ports could be reduced significantly. At an input pressure of 1 bar, only an output pressure of 0.53 bar was measurable at port A on the original part. With the final part, the output pressure was increased to 0.74 bar. For port B, an increase in the output pressure from 0.37 bar to 0.71 bar was possible.

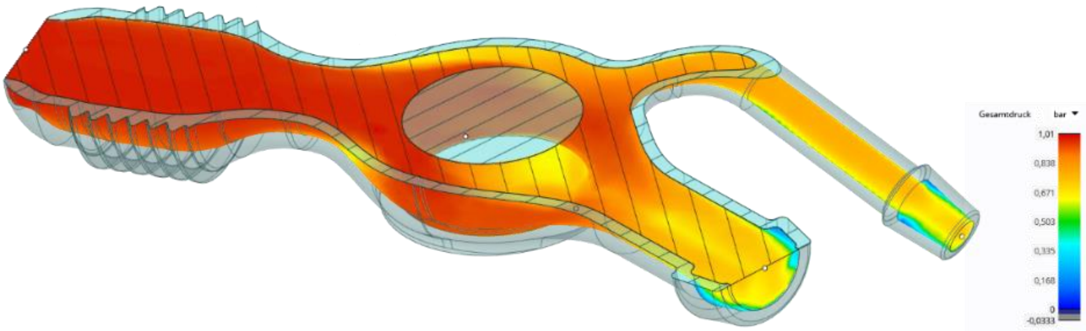

Figure 10: Flow simulation of version 12 - cutaway view

Figure 11 shows a comparison of the original version with the final version of the fuel collector. Next to the actual part, a sectional view is visible in each case. Here it is very easy to see how much material could be saved because the material thickness can be selected uniformly due to the LBM process. Only in the area of the functional surfaces minimally more material must be used so that the required surface quality can be realized after mechanical reworking. In addition, it is very clearly visible, especially in the sectional view, how much the flow properties could be optimized. All sharp edges have been rounded off and the diameter changes now also run smoothly and not abruptly, as it is the case with the original part.

Figure 11: Full view and sectional view of original part and version 12 of the fuel collector

4 Printing process and final overview

The additive manufacturing of the fuel collector was carried out on an EOS M280 with titanium powder (Ti6Al4V). Figure 12 shows the part in the powder bed on the left and the fully prepared part on the building platform on the right.

The original fuel collector consisting of 5 individual parts was adapted to a monolithic design, which has the following advantages:

- Reduced assembly costs
- No welded joints
- No weld inspection
- Flow optimization

The biggest advantage, however, is the weight reduction, which is shown in Table 2 by comparing the different materials and versions.

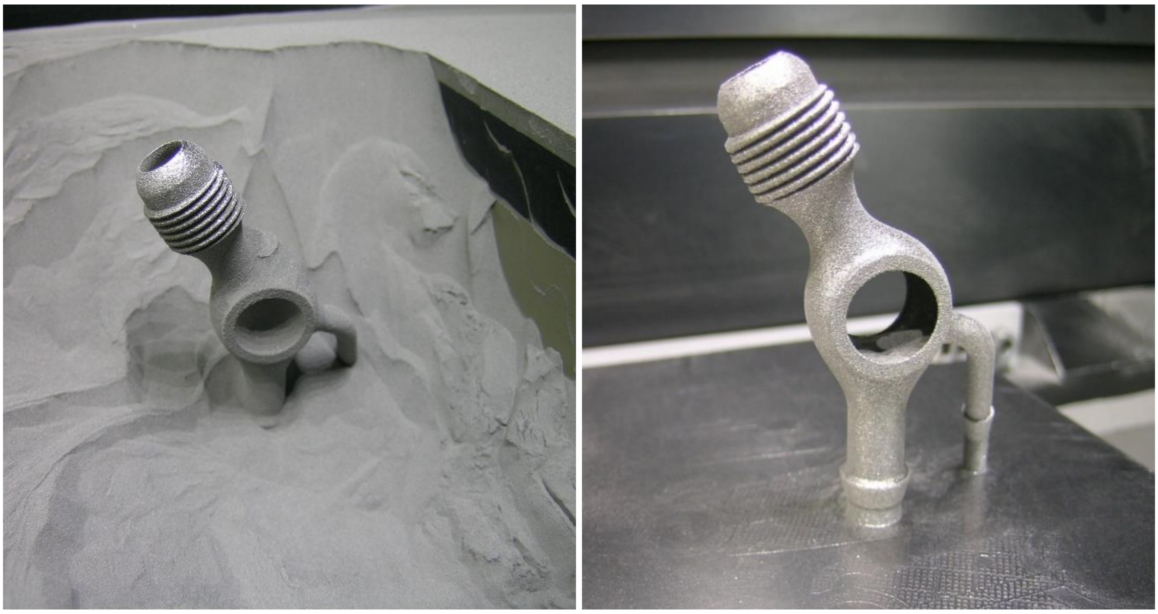

Figure 12: Fuel collector as version 12 on the building platform of the 3D printer

Table 2: Final overview of the volume and weight reduction of version 6 and 12

	original version	version 6		version 12	
material	stainless steel	stainless steel	Ti6Al4V	stainless steel	Ti6Al4V
volume	5,425 mm³	2,494 mm³		2,268 mm³	
volume reduction		- 55 %		- 59 %	
weight	43 g	20 g	11 g	18 g	10 g
weight reduction		- 55 %	- 74 %	- 59 %	- 77 %

An overview of the constructive changes of the individual versions can be seen in Figure 13, where the original version as well as the additively manufactured and finished reworked versions 6 and 12 are shown. The components were separated from the building platform and blasted in blasting chambers with corundum powder and stainless-steel beads to remove adhering powder particles and smooth the surface. This prevents particles from detaching from the surface at a later stage, where they can potentially cause damage.

Figure 14 shows the fuel collector as version 6 with connected tubes and fittings in the function test.

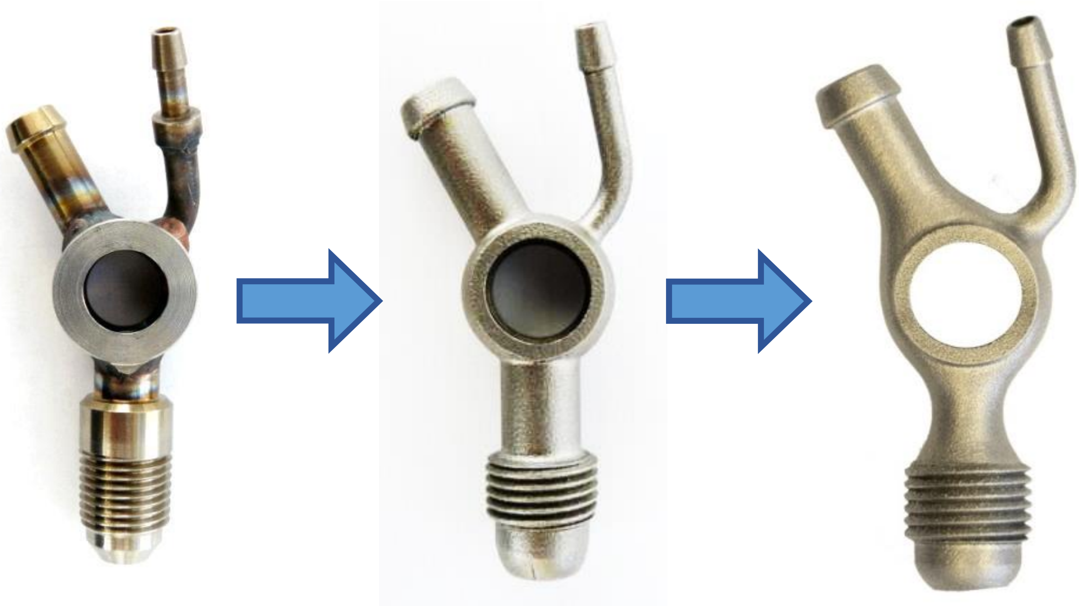

Figure 13: Manufactured fuel collector in original version (left), version6 (middle) and version 12 (right)

Figure 14: Fuel collector as version 6 with connected tubes and fitting

5 Quality assurance

UMMS PART is missing in this document.